Natural Resource Environment and Humans
No. 6. pp. 39–50. March 2016.

XRF analyses of major and trace elements in silicate rocks calibrated with synthetic standard samples

Hidehisa Mashima [1*]

Abstract

This paper describes techniques for calibrations of XRF analyses for major and trace elements in rock samples using synthetic standard samples. For major element analyses, standard samples were mixtures of pure reagents including analyzed elements. For trace element analyses, SiO_2 and SiO_2-TiO_2-$CaCO_3$ were used as major element matrices. Reagents including trace elements were stepwisely diluted with flux ($Li_2B_4O_7$). In spite of the compositional ranges of synthetic standards larger than those of natural rocks, calibration curves obtained in this study have high correlation coefficients and accuracies. Analytical results of JGS geochemical reference samples using obtained calibration curves show significant differences with their recommended values in several elements such as Y, Cr, Zr, Ni and V, which indicates that the recommended values of these elements have inaccuracies. Potential factors of the inaccuracies, such as earlier-generation experiments in the data set, are also discussed.

Keywords: X-ray fluorescence (XRF), the synthetic standard method, the diluted-flux method, JGS geochemical reference samples

Introduction

A dense database of geological and archeological obsidian is important for understanding of the relationships between natural resources and humans in the prehistoric period. In order to make a global obsidian database, precise analyses of rock samples are required. X-ray fluorescence spectrometry (XRF) is the method most frequently used for determinations of major and trace elements in silicate rock samples. A popular technique of the XRF calibration for trace element analyses in rock samples is that using commonsense values of geochemical standard samples (GRSs). However, developments of analytical methods other than XRF such as ICP-MS revealed that commonsense values of some elements such as Y are systematically different from analytical values determined using ICP-MS (e. g. Jochum and Jenner, 1994; Robinson et al., 1999), which is considered to be results of inaccurate XRF analyses calibrated using earlier-generation GRSs as standards.

In order to avoid systematic errors caused by inaccuracies of GRSs compositions, some laboratories calibrated XRF using synthetic samples made of reagents (Ichikawa et al., 1987; Mashima, 2002; Mori and Mashima, 2005). The synthetic standard method is adequate for making a global obsidian database since analytical results obtained from this method are independent of inaccuracies of GRSs compositions.

In this paper, I describe techniques of XRF calibrations using synthetic standard samples. Calibration curves for major and trace elements obtained using the synthetic standard method have high accuracies. Analyses of JGS GRSs using calibration curves obtained in this study revealed that recommended values of some trace elements would have significant inaccuracies. Potential factors causing inaccurate recommended values of JGS GRSs are also discussed.

Weighting conditions

A semi-micro analytical balance, A&D GH200, was used for weighting of reagents. Preciseness of weighting, one of the most important factors of the XRF calibration, depends on environments of experiments. Various factors, such as oscillation of the balance and static electricity charged on the sample, can cause weighing errors. At the start of this study,

1 Center for Obsidian and Lithic Studies, Meiji University, 370-8, Daimon, Nagawa-machi, Nagano 386-0601, Japan
* Corresponding author: H. Mashima (hmashima@meiji.ac.jp)

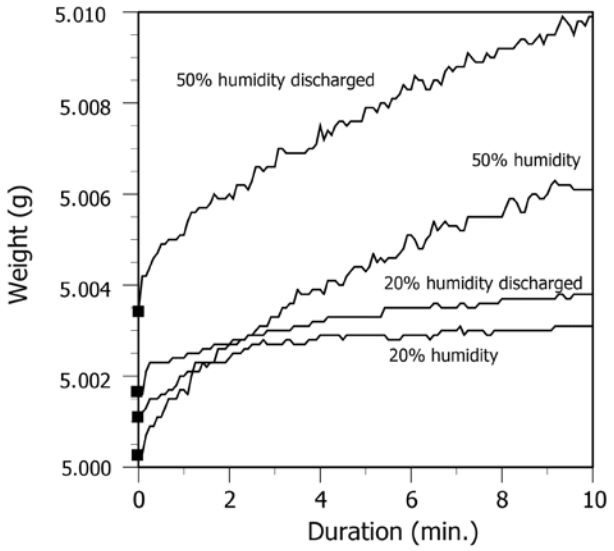

Figure 1 Duration changes in flux weights

however, provisions of these factors were insufficient. The balance was put on a plywood-working table and exposed to strong air current caused by an air conditioner and large temperature difference between the inside and the outside of the building. Since the laboratory is located at high altitude about 1400m, the air is strongly dry. The humidity of the laboratory was often lower than 30 % even though conventional humidifiers were used, which charged strong static electricity on samples. Because of these factors, the weighting results were unstable.

In order to get stable weighting results, I took several measures. The balance was laid on a weighting table, Sartorius YWT09, to minimize interfering vibration and flexure of the table. Air currents from the above and sides of the balance were broken by panels. The humidity of the laboratory was kept at around 50% to reduce electric charge of the sample and the operator during experiments. An increase of humidity, however, can cause weighting errors since reagents used in this study have moisture absorbency. For example, the weight of flux continues to increase even 10 minutes after the balance becomes steady (Fig. 1). Rapid weighting after the balance becomes steady therefore is required to make uncertain weighting error small. The static electricity was removed with corona discharge of the sample on the balance using a static eliminator, A&D AD-1683. Elimination of static electricity also makes removal of reagents from a charta ease. These provisions enabled us to get stable weighting results. Weighting results at the earlier stage of this study, however, could include errors caused by inadequate weighting conditions.

Table 1 Reagents used in this study

Reagent	Assay	Manufacture	Drying conditions	
			temperature	duration
SiO_2	99	Wako	1000 (°C)	10 (min)
TiO_2	99	Wako	600	30
Al_2O_3	99.9	Wako	1000	10
Fe_2O_3	99.9	Wako	600	30
MnO_2	99.5	Wako	RT	RT
MgO	99.9	Wako	600	60
$CaCO_3$	99.9	Wako	600	60
Na_2CO_3	99.8	Wako	600	60
K_2CO_3	99.5	Wako	600	90
KPOn		Wako	600	90
Sc_2O_3	99.9	Wako	600	60
NH_4VO_3	99	Wako	600	RT
Cr	99.5	Wako	600	RT
NiO	99.9	Wako	600	60
Rb_2SO_4	99	Wako	600	60
$SrCO_3$	99.99	Wako	600	60
Y_2O_3	99.99	Wako	600	60
ZrO_2	98	Wako	600	60
Nb_2O_5	99.9	Wako	600	60
$BaCO_3$	99.9	Wako	600	60
$Li_2B_4O_7$	99.9	Merck	600	60
LiI	99.9	Kojundo	RT	RT

Standard sample preparations

Standard samples for calibrations were synthesized from highly pure reagents shown in Table 1. Standards for major element determinations are mixtures of SiO_2, TiO_2, Al_2O_3, Fe_2O_3, MnO_2, MgO, $CaCO_3$, Na_2CO_3, K_2CO_3 and KPO_n. These reagents were weighted to make their total weight about 20 g and were mixed for 15 minutes using an agate mortar. A large deep-type mortar, with the inside diameter 140mm, the outside diameter 170 mm and the depth 50 mm, was used for well homogenization. The compositions of standard samples for major elements are listed in Table 2.

The duration for homogenization [15s] is short compared with that of previous studies [2 h] (Mashima, 2002; Mashima et al., 2002; Mori and Mashima, 2005). This is a result of

Table 2 Compositions of standard samples for major elements

	TN01	TN02	TN03	TN04	TN05	TN06	TN07	TN08	TN09	TN10
SiO_2	52.967	53.926	69.522	81.425	35.468	48.642	43.439	47.215	59.171	51.553
TiO_2	1.342	1.659	0.441	0.000	2.634	1.412	3.955	3.083	1.069	0.048
Al_2O_3	14.722	21.018	15.493	10.748	11.050	15.703	17.586	16.086	14.685	6.098
Fe_2O_3	9.112	7.039	2.686	0.000	14.872	12.390	18.847	15.495	8.949	13.419
MnO	0.152	0.131	0.112	0.000	0.510	0.092	0.797	0.493	0.149	0.050
MgO	7.809	2.507	1.147	0.187	15.194	7.690	2.987	4.249	5.091	27.927
CaO	9.370	7.408	2.790	0.000	12.865	11.094	6.148	7.602	5.595	0.905
Na_2O	2.807	4.065	4.038	3.150	4.862	2.708	2.735	3.115	2.940	0.000
K_2O	1.454	1.774	3.634	4.490	1.324	0.217	1.503	1.431	2.151	0.000
P_2O_5	0.264	0.474	0.136	0.000	1.223	0.051	2.001	1.233	0.200	0.000
Total	100.000	100.000	100.000	100.000	100.000	100.000	100.000	100.000	100.000	100.000
	TN11	TN12	TN13	TN14	TN15	TN16	TN17	TN18	TN19	TN20
SiO_2	64.501	56.380	50.092	74.401	50.955	65.460	48.837	75.309	49.402	48.506
TiO_2	0.656	0.297	0.113	0.093	0.515	0.000	0.815	0.057	2.397	1.210
Al_2O_3	15.125	11.725	30.774	12.317	8.761	19.152	3.521	14.582	12.243	14.179
Fe_2O_3	5.728	9.380	0.986	1.443	8.964	0.000	6.812	1.949	12.931	9.157
MnO	0.103	0.149	0.055	0.097	0.102	0.000	0.192	0.043	0.179	0.125
MgO	3.222	12.520	1.144	0.000	16.694	0.000	15.047	0.066	9.795	11.890
CaO	4.767	7.860	12.455	0.389	10.918	1.497	23.932	0.850	10.301	12.846
Na_2O	3.365	1.093	3.497	10.586	1.752	3.610	0.844	1.766	2.106	1.671
K_2O	2.392	0.397	0.851	0.674	1.132	10.282	0.000	5.378	0.418	0.270
P_2O_5	0.140	0.197	0.034	0.000	0.207	0.000	0.000	0.000	0.227	0.146
SiO_2	100.000	100.000	100.000	100.000	100.000	100.000	100.000	100.000	100.000	100.000

improvement of a pestle movement during homogenization. Precessional moving of a pestle effectively interchanges positions of reagents grains in a mortar, which significantly shortens the duration for the homogenization.

Reagents for trace elements calibrations were stepwisely diluted with flux (Merck Spectromelt A-10). In previous studies, the trace element reagents were divided into several groups. Reagents belonging to a group were mixed and diluted together (Mashima, 2002; Mashima and Mori, 2005). In this study, trace element reagents were individually diluted to evaluate interferences of slopes of X-ray peaks among them. At first, a reagent including 1 g of a trace element were mixed with 9 g of flux to make a diluted flux including 10 wt.% the element. Repeating this procedure diluted flux including 1 wt .%, 1000 ppm, 100ppm and 10 ppm of trace elements were prepared. In the trace element dilution, the digit number of essential figure was kept five, which is single-digit larger than that in the glass bead fusion.

In order to precise evaluations of mass absorption effects of major elements on trace elements analyses, a multi-major element matrix is adequate. However, a small amount of trace elements included as impurities in major element reagents could cause inaccurate calibration curves. For example, detectable Sr is included in $CaCO_3$ as an impurity (e.g. Ichikawa et al., 1987). In order to avoid this problem, two types of major element matrices were used for trace element calibrations. One is an SiO_2 matrix for calibrations of Nb, Zr, Y, Sr, Rb and Ni. The other is an SiO_2-TiO_2-$CaCO_3$ matrix for calibrations of V, Cr, Ba, Sc. TiO_2 were added to evaluate the line overlap Ti-Kα to V-Kα and Ba-Lα. $CaCO_3$ were done for estimation of the line overlap Ca-Kβ to Sc-Kα. TiO_2 and $CaCO_3$ for the matrix were stepwisely diluted with flux

similar to trace element reagents. Diluted flux with 10 wt. % and 1 wt.% of TiO_2 and $CaCO_3$ were prepared.

There are several methods to dilute trace element reagents. Robinson et al. (1999) diluted reagents with quartz. Because of high friction of quartz powders, it takes a long duration to make a mixture of a reagent and quartz homogeneous. An addition of trace element solution is an easy way to make a glass bead with trace elements (Goto et al., 2002). If trace element solutions added to a standard sample in a Pt-Au crucible, however, it is impossible to homogenize them well before fusion, which could cause compositional heterogeneities in a glass bead. If trace element solutions are added on a mortar, the amounts of added solutions could not be guaranteed by weighting on the balance because of the heaviness of a mortar, which leaves uncertainties of glass bead compositions. Nakayama and Nakamura (2005) proposed a diluted-glass bead method, whose concept is similar to the diluted-flux method in this study. The diluted-glass bead method fuses a mixture of trace element reagents and flux for homogenization, which could cause loss of elements during fusion although the loss volume is small. Compared with these methods, the diluted-flux method requires grate. The method, however, is simple. Qualities of experiments depend only on weighting. The duration of homogenization can be reduced with an adequate motion of the pestle and using an adequate size of a mortar. The diluted-flux method therefore is embraced in this study.

Glass bead preparations

Several ratios of a sample and flux, such as 1:10, 1:5 and 1:2, were proposed for analyses of major and trace elements in rock samples. The ratio 1:5 is embraced in this study from the viewpoints of X-ray intensities and the facility of a homogeneous glass bead preparation.

For major element calibrations, synthetic standards 1g converted to oxide weights and 5 g of flux were weighted on the balance respectively. 7 drops of LiI solution (about 300mg) were dropped on the flux to record the amount of added LiI. The weighted standard and flux were put in a mortar. For trace element charibarations, a major element matrix (SiO_2 ± diluted flux of TiO_2 and $CaCO_3$) and diluted flux of trace elements were weighted to make the total weight of oxides 1g and flux 5 g. After putting weighted reagents in a mortar, 10 drops of LiI solution (about 500mg) were added. Since glass beads for trace element calibrations have high SiO_2 contents, their melts are viscous and have affinity with an Au-Pt crucible. In order to steady exfoliation, the amount of the LiI added to glass beads for trace element calibrations is larger than that added to glass beads for major element calibrations.

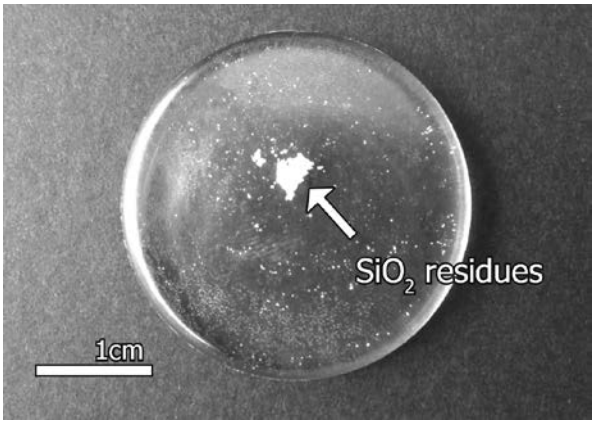

Figure 2 SiO_2 residues in a glass bead.

The reagent mixture was mixed to homogenize for a few minutes in an agate mortar. This process is important to make a homogeneous glass bead steady. Nakayama and Nakamura (2005) reported that preparation of glass beads was often failed when the solidified reagents remained. They considered that this is a result of insufficient mixing of reagents and flux. In this study, a failed glass was formed from an unhomogenized mixture when fusion clearing (Fig.2). Since the melting temperature of quartz is high (1650°C), it should be well dispersed in flux for steady fusion.

Nakayama and Nakamura (2005) also reported that the particle size of reagents affected performance of the glass beads. It is more serious for a rock samples composed of minerals various hardness. Coarse grains are sometimes remained in rock powder. During mixing in an agate mortar, sample powder is also grated, which reduces the grain size of it. Homogenization and grain refining in an agate mortar eases homogeneous glass bead preparations for various compositions.

Some researchers use a vibration touch mixer for the homogenization. (e.g. Tani et al., 2002; 2005). When I previously tried to use a touch mixer, however, heterogeneous beads were often made. A touch mixer is originally used for homogenization of an aqueous solution in which convection effectively occurs. Such well convection, however, does not occur in solid powder. Therefore, a powder mixture could not be thoroughly homogenized using a touch mixer. Tani et al. (2002, 2005) also put sample powder and flux in a crucible before homogenization to avoid using a charta for precise weighting. As mentioned above, however, elimination of static makes powder removal from charta ease. Precise weighting therefore is possible if a charta is in equilibrium with atmosphere in term of humidity before experiments.

Thoroughly homogenized reagents were fused in a crucible made of Pt alloys with oxide particles and Au manufactured

Table 3 Instrumental conditions of the XRF spectrometer

	Line	Slit	Crystal	Detector	Angle 2θ(°)			Counting time			PHA	
					Peak	BG1	BG2	peak	BG1	BG2	lower	upper
SiO_2	Si-Kα	S4	PET	PC	109.03	96.95	115.00	10	5	5	120	280
TiO_2	Ti-Kα	S2	LiF200	SC	86.14	84.54	88.12	20	10	10	150	250
Al_2O_3	Al-Kα	S4	PET	PC	144.77	140.00	148.00	20	10	10	120	280
Fe_2O_3	Fe-Kα	S2	LiF200	SC	57.50	56.44	58.30	10	5	5	120	300
MnO	Mn-Kα	S2	LiF200	SC	62.98	61.98	63.98	20	10	10	150	250
MgO	Mg-Kα	S4	RX25	PC	37.95	34.35	43.25	60	30	30	150	270
CaO	Ca-Kα	S4	LiF200	PC	113.12	110.12	116.62	10	5	5	150	250
Na_2O	Na-Kα	S4	RX25	PC	46.51	44.00	48.00	60	30	30	150	250
K_2O	K-Kα	S4	LiF200	PC	136.65	128.00	145.20	10	5	5	1150	250
P_2O_5	P-Kα	S4	Ge	PC	141.05	136.05	144.75	40	20	20	150	250
Sc	Sc-Kα	S4	LiF200	PC	97.75	96.72	98.73	120	60	60	100	300
V	V-Kα	S2	LiF200	SC	76.91	76.49	77.92	100	50	50	100	300
Cr	Cr-Kα	S2	LiF200	SC	69.33	68.66	70.43	60	30	30	100	300
Ni	Ni-Kα	S2	LiF200	SC	48.62	48.22	49.18	60	30	30	120	300
Rb	Rb-Kα	S2	LiF200	SC	26.58	26.12	27.28	60	30	30	120	280
Sr	Sr-Kα	S2	LiF200	SC	25.12	24.66	26.00	60	30	30	120	280
Y	Y-Kα	S2	LiF200	SC	23.78	23.12	24.36	60	30	30	120	270
Zr	Zr-Kα	S2	LiF200	SC	22.52	22.14	23.12	60	30	30	120	270
Nb	Nb-Kα	S2	LiF200	SC	21.36	20.88	21.80	60	30	30	120	280
Ba	Ba-Lα	S2	LiF200	SC	87.13	88.02		100	100		100	300
I	I-Lα	S4	LiF200	SC	102.92	101.60	104.35	40	20	20	100	300

by Furuya metal. A desktop bead sampler manufactured by Rigaku was used for heating. Heating conditions are flowing, pre-heating at 950°C for 120s, main heating 1200°C for 240s, heating with agitation at 1200°C for 300s. Each prepared glass bead was put in a plastic back and kept in a desiccator.

It is worth to mention here that an increase of a blank level was observed on Ni after making a bead containing more than 1000 ppm Ni (Fig. 3). This would have been a result of a reaction between Ni in a reagent mixture and Pt in a crucible. In order to decrease the blank level to the initial condition, more than ten times flux-fusions were required for the contaminated crucible. A blank check therefore is recommend after making glass beads of ultramafic samples with high Ni contents.

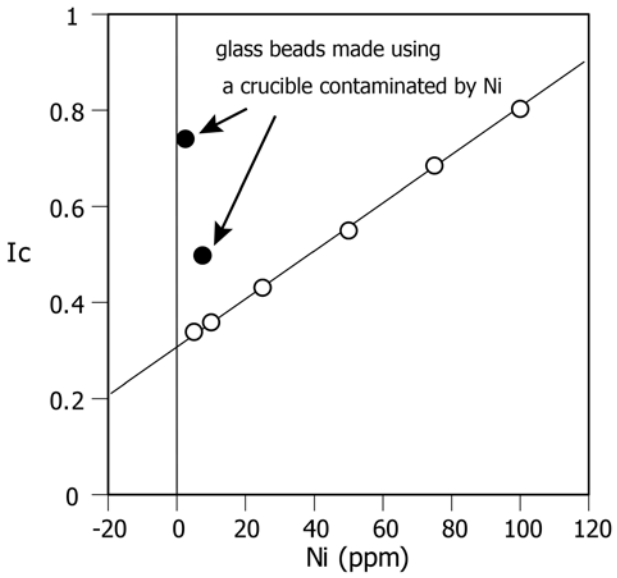

Figure 3 Contamination of Ni from a Pt-Au crucible.

Table 4 Coefficients of correlation and accuracies of calibration curves

component	composition range	correlation coefficient	accuracy
SiO_2	35.468 – 81.425 (wt.%)	0.99954	0.37 (wt.%)
TiO_2	0 - 3.955	0.99995	0.012
Al_2O_3	3.521 - 19.152	0.99982	0.11
Fe_2O_3	0 - 18.847	0.99995	0.057
MnO	0 - 0.510	0.99997	0.0018
MgO	0 - 27.927	0.99991	0.085
CaO	0 - 23.932	0.99992	0.081
Na_2O	0 - 10.586	0.99990	0.045
K_2O	0 - 10.282	0.99974	0.058
P_2O_5	0 - 2.001	0.99996	0.0047
Sc	0 – 100.0 (ppm)	0.99979	0.81 (ppm)
V	0 - 1000	0.99906	4.3
Cr	0 - 3000	0.99999	3.8
Ni	0 - 10.00	0.97450	1.3
	10.00 - 100.0	0.99990	0.73
	100.0 - 3000	0.99998	7.2
Rb	0 - 500.0	0.999999	0.63
Sr	0 - 2000	0.999999	1.4
Y	0 - 100.0	0.99999	0.37
Zr	0 - 500.0	0.99995	2.9
Nb	0 - 100.0	0.99985	0.31
Ba	0 - 100.0	0.92538	8.2
	100.0 - 875.0	0.99995	4.3
	875.0 - 2874	0.99937	41

Instrumental conditions

A wavelength dispersive X-ray florescence spectrometer used in this study was Rigaku ZSX Primus III+ at the Center for Obsidian and Lithic Studies. The excitation source is an end-window 3 kW Rh anode operated at 50 kV and 50mA. X-ray dispersive crystals were RX25, PET, Ge and LiI (200). Detectors were a flow proportional counter (F-PC) for light elements and scintillation counter (SC) for heavy elements. PR gas flowed in F-PC at 50 cm^3/min. During determinations, the temperature of the monochromator chamber was kept at 36.5 C. Other instrumental conditions are listed in Table 3.

Calibration curves

Calibration lines were empirically evaluated using a general formula.

$$\mathrm{Wi} = (AIi^3 + BIi^2 + CIi + \mathrm{D})(1 + \sum AijFj) + \sum BijFj \quad (1)$$

Where *Wi* is a quantitative value of an element (oxide) *i*. *Ii* is a X-ray intensity of element i; A, B and C coefficients of a calibration curve; D a constant term; *Aij*, a coefficient for mass absorption and excitation of element j for I; *Bij*, a coefficient for an overlap interference of j for I; *Fj* a concentration or an X-ray intensity of j.

Mori and Mashima (2005) mentioned that the line overlap

Table 5 Analytical results of GJS geochemical standard samples

	JA-1			JA-2			JA-3			JB-1a		
	RV	RVn	result	RV	RVn	result	RV	RVn	result	RV	RVn	result
SiO_2 (wt. %)	63.97	64.41	64.51	56.42	57.71	57.35	62.27	62.33	62.23	52.41	53.01	53.05
TiO_2	0.85	0.86	0.85	0.66	0.68	0.68	0.7	0.70	0.67	1.28	1.29	1.30
Al_2O_3	15.22	15.33	15.52	15.41	15.76	16.04	15.56	15.57	16.01	14.45	14.62	14.90
Fe_2O_3*	7.07	7.12	7.03	6.21	6.35	6.38	6.6	6.61	6.52	9.05	9.15	9.00
MnO	0.157	0.158	0.15	0.108	0.110	0.11	0.104	0.104	0.10	0.148	0.150	0.14
MgO	1.57	1.58	1.54	7.6	7.77	7.90	3.72	3.72	3.68	7.83	7.92	7.96
CaO	5.7	5.74	5.69	6.29	6.43	6.37	6.24	6.25	6.24	9.31	9.42	9.32
Na_2O	3.84	3.87	3.86	3.11	3.18	3.17	3.19	3.19	3.16	2.73	2.76	2.77
K_2O	0.77	0.78	0.81	1.81	1.85	1.90	1.41	1.41	1.45	1.4	1.42	1.47
P_2O_5	0.165	0.166	0.16	0.146	0.149	0.15	0.116	0.116	0.11	0.26	0.26	0.26
	99.31	100.00	100.13	97.76	100.00	100.05	99.91	100.00	100.18	98.87	100.00	100.17
Sc (ppm)	28.5	28.7	28	19.6	20.0	19.0	22	22	21	27.9	28.2	30
V	105	106	110	126	129	129	169	169	174	205	207	208
Cr	7.83	7.88	-	436	446	471	66.2	66.3	66	392	396	424
Ni	3.49	3.51	-	130	133	139	32.2	32.2	28	139	141	135
Rb	12.3	12.4	14	72.9	74.6	75	36.7	36.7	37	39.2	40	40
Sr	263	265	261	248	254	250	287	287	286	442	447	453
Y	30.6	30.8	26	18.3	18.7	15.0	21.2	21	18	24	24	21
Zr	88.3	88.9	85	116	119	117	118	118	117	144	146	145
Nb	1.85	1.9	1	9.47	9.69	8.00	3.41	3	2	26.9	27	26
Ba	311	313	317	321	328	318	323	323	331	504	510	510

RV: recommended values (Imai et al., 1995), RVn: recommended values normalized to make total of major elements 100 wt.%

correction of I-Lβ_2 is not required. In this study, however, the amount of added LiI (300 mg) is three times larger than that in Mori and Mashima (2005). A meaningful peak of I-Lβ_2 is observed near Ti-Kα. Therefore, a line overlap correction of I-Lβ_2 using I-Lα was carried out for TiO_2 determination.

Instead of a net intensity, a corrected intensity, the ratio of a net intensity to a background intensity, was used for evaluations of calibration curves for trace elements to correct mass absorption effects. The general formula for calibration curves of trace elements is written as:

$$\mathrm{Wi} = AIci^3 + BIci^2 + CIci + \mathrm{D} + \sum BijFj \qquad (2)$$

Where *Ici* is a corrected X-ray intensity of element i

Conventional line overlap corrections were carried out for Sc, V, Cr, Y, Zr, Nb and Ba similar to Mashima (2002). Calibration lines of Ni and Ba were divided into three intervals to keep high accuracy for low concentration samples. Coefficients of correlation and accuracy of calibration lines are shown in Table 4. Due to time constraints, detected limits of trace elements could not be investigated.

Results of GSJ GRSs measurements

Major and trace element contents in GSJ geochemical reference samples (GRSs) were determined using calibration curves obtained in this study. In order to check complete decompositions of samples, I designed the analyses to be anhydrous. About 5 g of the samples therefore were heated at 950 °C for 1 hour for oxidization and dehydration before fusion. Analytical results of GSJ GRSs are shown in Table 5. The composition is an average of three times determinations.

For major elements, analytical results of GRSs are close to their recommended values normalized to make the total of major elements 100 wt. %. The total of major element

(continued)

	JB-2			JB-3			JF-1			JG-1a		
	RV	RVn	result	RV	RVn	result	RV	RVn	result	RV	RVn	result
SiO_2 (wt. %)	53.25	52.96	52.80	50.96	50.77	50.68	66.69	67.25	67.34	72.3	72.91	73.05
TiO_2	1.19	1.18	1.16	1.44	1.43	1.43	0.005	0.01	0.00	0.25	0.25	0.23
Al_2O_3	14.64	14.56	14.74	17.2	17.13	17.49	18.08	18.23	18.49	14.3	14.42	14.58
Fe_2O_3*	14.25	14.17	14.04	11.82	11.78	11.69	0.08	0.08	0.05	2	2.02	1.93
MnO	0.218	0.22	0.21	0.177	0.18	0.17	0.001	0.00	0.00	0.057	0.06	0.06
MgO	4.62	4.59	4.68	5.19	5.17	5.22	0.006	0.01	0.00	0.69	0.70	0.68
CaO	9.82	9.77	9.64	9.79	9.75	9.65	0.93	0.94	0.88	2.13	2.15	2.10
Na_2O	2.04	2.03	1.95	2.73	2.72	2.69	3.37	3.40	3.25	3.39	3.42	3.39
K_2O	0.42	0.42	0.46	0.78	0.78	0.81	9.99	10.07	10.03	3.96	3.99	3.89
P_2O_5	0.101	0.10	0.10	0.294	0.29	0.30	0.01	0.01	0.01	0.083	0.08	0.08
	100.54	100.00	99.77	100.38	100.00	100.13	99.16	100.00	100.05	99.16	100.00	99.98
Sc (ppm)	53.5	53.2	52	33.8	33.7	34	0.23	0.23	-	6.21	6.26	4
V	575	572	580	372	371	388	5.43	5.48	-	22.7	22.9	14.0
Cr	28.1	27.9	17	58.1	57.9	55	5.48	5.53	-	17.6	17.7	17.0
Ni	16.6	16.5	8	36.2	36.1	33	1.36	1.37	1	6.91	6.97	3
Rb	7.37	7.33	7	15.1	15.0	15	266	268	279	178	180	190
Sr	178	177	177	403	401	406	172	173	165	187	189	182
Y	24.9	24.8	21	26.9	26.8	24	2.84	2.86	-	32.1	32.4	28
Zr	51.2	50.9	47	97.8	97.4	98	38.6	38.9	35	118	119	130
Nb	1.58	2	0	2.47	2	2	0.74	1	-	11.4	11.5	8
Ba	222	221	230	245	244	243	1750	1765	2007	470	474	501

concentrations tend to be slightly larger than 100 wt. %. Since the GRSs contain trace elements, the total of their major element contents should be smaller than 100 wt. %. The reason of this phenomenon has not been understood yet.

For trace elements, analytical results of Sc, Rb, Sr and Nb are close to normalized recommended values (RVn) of them. The analytical results of Y are 2.3 – 8 ppm lower than the RVns of Y. The determined Cr in JA-2 (471 ppm) and JB-1a (424 ppm) is meaningfully higher than the RVns (446 ppm for JA-1 and 396 ppm for JB-1a), whereas Cr in JGb-1 (47 ppm) is 11.2 ppm lower than its RVn (58.2 ppm). The Ni contents of JA-3 (28 ppm), JB-2 (8 ppm) and JB-3 (33 ppm) are meaningfully lower than the RVns (JA-3 = 32.2 ppm, JB-2 = 16.5 ppm, JB-3 = 36.1 ppm). The Zr contents in granitic GRSs such as JG-1a, JG-2, and JG-3 are higher than the RVns, 119 ppm for JG-1a, 98.3 ppm for JG-2 and 145 for JG-3. V in JG-1a (14 ppm) is lower than the RVn (22.9 ppm). The determined Ba tends to be higher than the RVns.

Discussions

Incongruities in yttrium

In determinations of GSJ GRSs, a systematic difference is observed between the analytical results and RVns in yttrium (Fig. 4a). In this study, an SiO_2 matrix was used for the calibration of the Y determination. Similar systematic difference, however, was observed my previous calibration using multi-major element matrices (Mashima, 2002). The difference, therefore, is essential. Similar systematic difference of analytical results was also observed between ICP-MS and XRF (e.g. Jochum and Jenner, 1994; Robinson et al., 1999). Jochum and Jenner (1994) considered that this is inaccuracies of RVs of GSJ GRSs depending on earlier-generation analyses.

(continued)

	JG-2			JG-3			JR-1			JR-2		
	RV	RVn	result	RV	RVn	result	RV	RVn	result	RV	RVn	result
SiO_2 (wt. %)	76.83	77.36	77.51	67.29	67.82	67.92	75.45	76.51	76.57	75.69	76.96	76.98
TiO_2	0.044	0.04	0.04	0.48	0.48	0.47	0.11	0.11	0.10	0.07	0.07	0.05
Al_2O_3	12.47	12.56	12.81	15.48	15.60	15.92	12.83	13.01	13.02	12.72	12.93	12.85
Fe_2O_3*	0.97	0.98	0.89	3.69	3.72	3.65	0.89	0.90	0.86	0.77	0.78	0.73
MnO	0.016	0.02	0.01	0.071	0.07	0.07	0.099	0.10	0.10	0.112	0.11	0.12
MgO	0.037	0.04	0.04	1.79	1.80	1.78	0.12	0.12	0.12	0.04	0.04	0.05
CaO	0.7	0.70	0.69	3.69	3.72	3.70	0.67	0.68	0.71	0.5	0.51	0.53
Na_2O	3.54	3.56	3.53	3.96	3.99	4.03	4.02	4.08	4.02	3.99	4.06	4.04
K_2O	4.71	4.74	4.40	2.64	2.66	2.62	4.41	4.47	4.70	4.45	4.52	4.83
P_2O_5	0.002	0.00	0.00	0.122	0.12	0.13	0.021	0.02	0.02	0.012	0.01	0.01
	99.319	100.00	99.93	99.213	100.00	100.28	98.62	100.00	100.21	98.354	100.00	100.18
Sc (ppm)	2.42	2.44	2	8.76	8.83	7	5.07	5.14	4	5.59	5.68	7
V	3.78	3.81	-	70.1	70.7	69	7	7	-	3	3	-
Cr	6.37	6.41	-	22.4	22.6	20	2.83	2.87	-	3.1	3.2	-
Ni	4.35	4.38	1	14.3	14.4	11	1.67	1.69	-	1.99	2.0	-
Rb	301	303	309	67.3	67.8	75	257	261	269	303	308	317
Sr	17.9	18.0	13	379	382	371	29.1	30	26	8.11	8	5
Y	86.5	87.1	80	17.3	17.4	14	45.1	46	39	51.1	52	44
Zr	97.6	98.3	113	144	145	164	99.9	101	100	96.3	97.9	97
Nb	14.70	14.8	9	5.88	5.9	3	15.20	15	11	18.70	19	13
Ba	81	82	67	466	470	495	50.3	51.0	66	39.5	40.2	37

As shown in Fig. 4b, however, the systematic difference is also observed between the results of this study and those of Mori and Mashima (2002) although they used the synthetic standard method for XRF calibrations. Mori and Mashima (2002) used multi-major element matrices for calibrations of trace element determinations. As mentioned above, however, a major element matrix would not be the reason of the systematic difference. This study and Mashima (2002) used the background-intensity method to correct mass absorption effects. Calibration curves obtained using this method are expressed by the equation (2).

$$\mathrm{Wi}=AIci^{3}+BIci^{2}+CIci+\mathrm{D}+\sum BijFj \qquad (2)$$

Mori and Mashima (2005) used the de Jongh model, which is expressed with an equation

$$\mathrm{Wi}=(CIi+\mathrm{D})(1+\sum AijFj)+\sum BijFj \qquad (3)$$

$$\mathrm{Wi}=CIi+CIi\sum AijFj+\mathrm{D}+\mathrm{D}\sum AijFj+\sum BijFj \qquad (3)'$$

In the case of $A = B = 0$ in eq. (2), *Ici* has the same mean $CIi\sum AijFj$ in the eq. (3)', since both of them are intensities corrected about mass absorption effects. The eq. (3)' contain an uncorrected intensity term *CIi*, which would reduce the effect of the correction of the line overlap of Rb-Kβ on the Y determination. If this is the case, an inadequate selection of the model for the evaluation of mass absorption effects would cause an inaccurate determination of Y. This interpretation should be verified in future researches.

Incongruities in other elements

The determined Cr contents in JA-1 and JB-1a are significantly higher than those RVns. A typical reservoir of Cr in igneous rocks is a spinel. JA-1 and Jb-1a contain spinels as inclusions in mafic phenocrysts. Although JB-1 (Cr RV =

(continued)

	JGb-1		
	RV	RVn	result
SiO_2 (wt. %)	43.66	43.99	44.11
TiO_2	1.6	1.61	1.60
Al_2O_3	17.49	17.62	17.74
Fe_2O_3*	15.06	15.17	15.15
MnO	0.189	0.19	0.19
MgO	7.85	7.91	8.13
CaO	11.9	11.99	11.84
Na_2O	1.2	1.21	1.17
K_2O	0.24	0.24	0.26
P_2O_5	0.056	0.06	0.05
	99.245	100.00	100.24
Sc (ppm)	35.8	36.1	38
V	635	640	636
Cr	57.8	58.2	47
Ni	25.4	25.6	21
Rb	6.87	6.92	10
Sr	327	329	326
Y	10.4	10	7
Zr	32.8	33.0	30
Nb	3.34	3	-
Ba	64.3	64.8	74

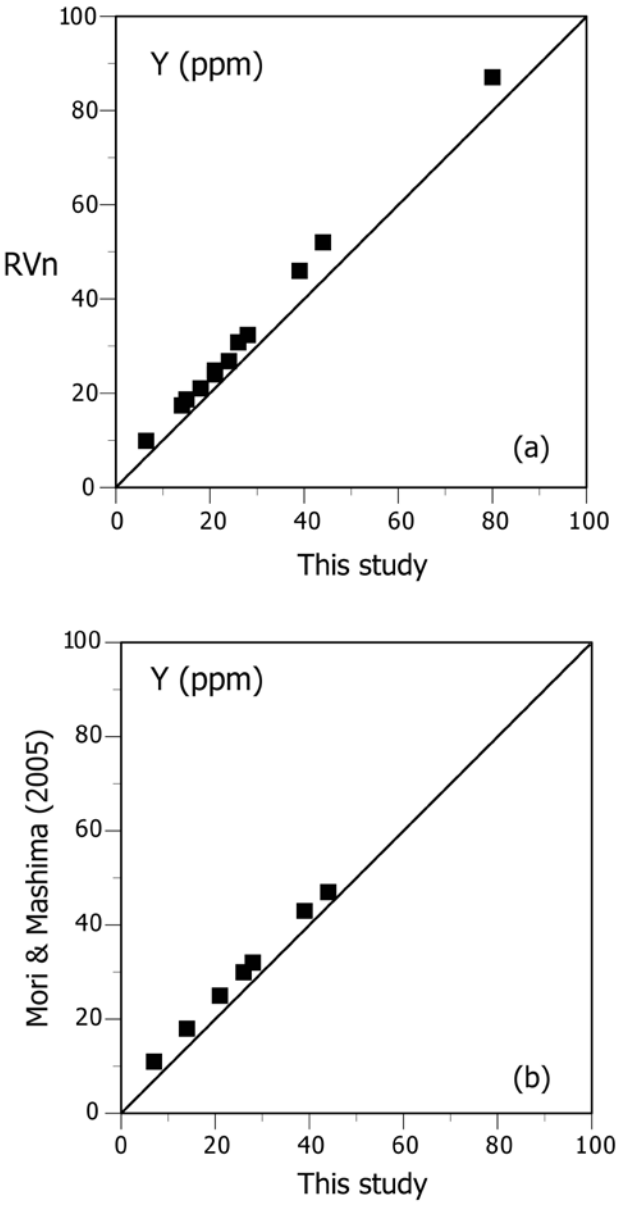

Figure 4 Incongruities of analytical results of Y. (a) incongruities between this study and normalized recommended values, (b) incongruities between this study and Mori and Mashima (2005).

425 ppm), JB-1a (Cr Rv = 392 ppm) and JB-1b (Cr RV = 439 ppm) were collected from the same outcrop, the Cr RV of JB-1a is significantly lower than those of JB-1 and JB-1b. Since spinel is a highly refractory mineral, the incongruities between results of this study and the RVns would be caused by an incomplete decomposition of spinel in previous experiments used evaluations of the Cr RVs. In Mashma (2002), the GRSs were fused at 1050 °C, which leaded to a low analytical result of Cr in JB-1a (380 ppm). In later analysis of basaltic samples, I found that a high temperature condition is required to decompose spinels in mafic rocks. In this study, therefore, the GRSs were fused at 1200 °C.

A similar difference is observed in the Zr contents in granitic GRSs (JG-1a, JG-2 and JG-3). Zircon, the main reservoir of Zr in granitic rocks, however, is easily decomposed by fusion. The Zr content in JG-1a fused at 1050 °C (129 ppm) in Mashima (2002) is similar to that obtained in this study (130 ppm). The data for the Zr RVs of granitic GRSs contains many results obtained using XRF calibrated with the earlier-generation GRSs, which would cause inaccurate RVs of Zr for granitic GRSs. Determined Ni (8 ppm) in JB-2 and V (14 ppm) in JG-1a are significantly lower than their RVns (Ni = 16.5 ppm for JB-2, V = 22.9 ppm for JG-1a). These incongruities would also be the results of inaccuracies in the RVs of the GRSs, since the data sets of these RVs also contain numbers of values obtained from XRF calibrated with earlier-generation GRSs. In order to determine

trace elements in low concentrations, their blank intensities should be measured. The calibration using GRSs as standards, however, could not do it.

Conclusion

In this paper, I examined calibration techniques for XRF analyses of major and trace elements in rock samples using synthetic standards. This study realized highly-accurate XRF analyses independent of geochemical standard samples (GRSs) and other laboratories, which gives a robust basis for geochemical and geoarcheological investigations. The techniques presented in this paper would also give benefits to other analytical methods such as ICP-MS. Double check between XRF and such analytical methods would improve reliabilities of analytical results.

This study revealed that recommended values of several trace elements in JGS GRSs still have significant inaccuracies. XRF analyses using JGS GRSs as standards therefore have significant systematic errors even if their calibration curves have high accuracies. The synthetic standard method is the most convenience way for a precise XRF calibration, since the method does not require additional tools other than efforts of researchers.

Acknowledgements

I thank anonymous reviewers whose comments improved this paper. This study was partly supported by the Supported Program for the Strategic Research Foundation at Private Universities, 2011-2016 (S1101921) by the MEXT.

References

Goto, A., Horie, T., Ohba, T. and Fujimaki, H. 2002 XRF analysis of major and trace elements for wide compositional ranges from silicate rocks to carbonate rocks using low dilution glass beads. *Japanese Magazine of Mineralogical and Petrological Sciences* 31: 162-173.

Ichikawa, H., Sakai, T. and Watanabe, T. 1987 Quantitative analysis of seven trace elements in silicate rocks using fused disk-samples by X-ray fluorescence method (Rh-tube). *Geological Reports, Shimane University* 6: 161-169.

Imai, N., Terashima, S., Itoh S. and Ando, A. 1995 1994 compilation values for JGS reference samples “Igneous rock series”. *Geochemical Journal* 29: 91-95.

Jochum, K. P. and Jenner, G. 1994 Trace element analysis of Geological Survey of Japan silicate reference materials: Comparison of SSMS with ICP-MS data and a critical discussion of compiled values. *Fresenius' Journal of Analytical Chemistry* 350: 310-318.

Mashima, H. 2002 Improvement of XRF analysis for trace elements in silicate rock samples using the flux-fused disk method. *Science Reports, Department of Earth and Planetary Sciences, Kyushu University* 21: 37-48.

Mashima, H., Maeda, S., Takahashi, Y., Sato, N. and Ide, T. 2002 Re-examination of XRF analyses for major element compositions of silicate rock samples. *Science Reports, Department of Earth and Planetary Sciences, Kyushu University* 21: 27-35.

Mori, Y., Mashima, H. X-ray fluorescence analysis of major and trace elements in silicate rocks using 1:5 dilution glass beads. *Bulletin of Kitakyushu Museum of Natural History and Human History, Series A (Natural History)* 3: 1-12.

Nakayama, K. and Nakamura, T. 2005 X-ray fluorescence analysis of rare earth elements in rocks using low dilution glass beads. *Analytical Science* 21: 815-822.

Robinson, P., Townsend A.T., Yu, Z. and Munker, C. 1999 Determination of scandium, yttrium and rare earth elements in rocks by high resolution inductively coupled plasma-mass spectrometry. *Geostandards Newsletter* 23: 31-46.

Tani, K., Kawabata, H., Chang, Q., Sato, K. and Tatsumi, Y. 2005 Quantitative analyses of silicate rock major and trace elements by X-ray fluorescence spectrometer: Evaluation of analytical precision and sample preparation. *Frontier Research on Earth Evolution* 2: 1-8.

Tani, K., Orihashi, Y. and Nakada, S. 2002 Major and trace component analysis of silicate rocks using fused glass bead by X-ray fluorescence spectrometer: Evaluation of analytical precision for third, sixth and eleventh dilution fused glass beads. *Technical Research Report, Earthquake Research Institute, University of Tokyo* 8: 26-36.

(Received 19 February 2016/ Accepted 18 March, 2016)

資源環境と人類　第 6 号　39–50 頁　2016 年 3 月
Natural Resource Environment and Humans
No. 6.　pp. 39–50.　March 2016

合成標準試料を用いて校正した岩石の主成分及び微量成分元素の XRF 分析

眞島英壽 [1*]

要　旨

本論文では蛍光 X 線分析装置による岩石の主成分及び微量成分元素分析について，合成標準試料を用いた校正方法について記述する．主成分元素分析に用いた標準試料は分析元素を含む高純度試薬を混合して調合した．微量元素分析には SiO_2 マトリックスと SiO_2-TiO_2-$CaCO_3$ マトリックスの二つを主成分マトリックスとして用いた．微量元素を含む試薬は融剤（$Li_2B_4O_7$）によって段階的に希釈した．天然の岩石よりも広い組成範囲の標準試料を準備したにもかかわらず，本研究で得られた検量線は高い相関係数と正確度を示した. 得られた検量線を用いて JGS 地質標準試料の分析を行ったところ, イットリウム，クロム，ジルコニウム，ニッケルおよびバナジウムについて，分析結果と推奨値の間に明確な違いが認められた．これらの元素の推奨値に不正確さがあると考えられる．技術的に旧世代の実験など考えられる地質標準試料推奨値の不正確さの原因について考察した.

キーワード：蛍光 X 線分析，合成標準試料法，融剤希釈法，JGS 地質標準試料

（2016 年 2 月 19 日受付／ 2016 年 3 月 18 日受理）

1　明治大学黒耀石研究センター　〒 386-0601 長野県小県郡長和町大門 3670 - 8
＊　責任著者：眞島英壽（hmashima@meiji.ac.jp）